

Cite this: *Chem. Sci.*, 2015, 6, 1747

# Design of an intelligent sub-50 nm nuclear-targeting nanotheranostic system for imaging guided intranuclear radiosensitization†

Wenpei Fan,<sup>a</sup> Bo Shen,<sup>b</sup> Wenbo Bu,<sup>\*a</sup> Xiangpeng Zheng,<sup>c</sup> Qianjun He,<sup>a</sup> Zhaowen Cui,<sup>a</sup> Kuaile Zhao,<sup>d</sup> Shengjian Zhang<sup>d</sup> and Jianlin Shi<sup>\*a</sup>

Clinically applied chemotherapy and radiotherapy is sometimes not effective due to the limited dose acting on DNA chains resident in the nuclei of cancerous cells. Herein, we develop a new theranostic technique of "intranuclear radiosensitization" aimed at directly damaging the DNA within the nucleus by a remarkable synergetic chemo-/radiotherapeutic effect based on intranuclear chemodrug-sensitized radiation enhancement. To achieve this goal, a sub-50 nm nuclear-targeting rattle-structured upconversion core/mesoporous silica nanotheranostic system was firstly constructed to directly transport the radiosensitizing drug Mitomycin C (MMC) into the nucleus for substantially enhanced synergetic chemo-/radiotherapy and simultaneous magnetic/upconversion luminescent (MR/UCL) bimodal imaging, which can lead to efficient cancer treatment as well as multi-drug resistance circumvention *in vitro* and *in vivo*. We hope the technique of intranuclear radiosensitization along with the design of nuclear-targeting nanotheranostics will contribute greatly to the development of cancer theranostics as well as to the improvement of the overall therapeutic effectiveness.

Received 8th October 2014  
Accepted 5th December 2014

DOI: 10.1039/c4sc03080j

[www.rsc.org/chemicalscience](http://www.rsc.org/chemicalscience)

## 1 Introduction

During the past decades, chemotherapy has achieved great success in relieving the pain of tumor patients and extending their lifetime. However, it is difficult to further improve the overall treatment efficacy because of unspecific drug delivery. What is worse, most patients may develop multi-drug resistance (MDR) after frequent administration of free drugs.<sup>1</sup> MDR, arising from the over-expression of the drug efflux P-glycoprotein (P-gp) pumps, has become one of the major challenges of cancer chemotherapy.<sup>2</sup> Although various drug delivery systems (DDSs) have been reported to be capable of reversing MDR to some extent by improving the cellular drug accumulation,<sup>1b</sup> most of the released drugs within the cell cytoplasm fail to enter the nucleus, which inevitably lowers the chemotherapeutic effectiveness. Therefore, more advanced drug delivery strategies, such as intranuclear drug delivery, are in urgent need for effective anti-MDR.

In addition, radiotherapy can also efficiently kill MDR cells by focusing high-energy X-ray radiation on them to damage the DNA chains.<sup>3</sup> However, most solid tumors are in lack of oxygen as compared to normal tissues, which often causes the failure of radiotherapy.<sup>4</sup> Fortunately, some representative anticancer drugs, such as Mitomycin C (MMC), are selectively toxic to hypoxic solid tumors. MMC can be activated by the reducing (hypoxic) environment to inhibit DNA synthesis. More importantly, MMC can simultaneously serve as a radiosensitizer to enhance radiotherapy efficacy.<sup>5</sup> Therefore, the combined use of MMC and X-ray radiation may contribute to the improved effectiveness of cancer therapeutics.<sup>6</sup> Previous studies mainly focused on extracellular radiosensitization (free drugs and radiotherapy)<sup>7</sup> or intracytoplasmic radiosensitization (intracytoplasmic delivered drugs and radiotherapy),<sup>8</sup> which failed to achieve the optimized treatment efficacy because few drugs can passively diffuse into the cell nucleus to synergistically enhance the radiotherapy efficacy on breaking down the DNA. Therefore, the design of an active nuclear-targeting drug vehicle that can efficiently transport MMC into the nucleus<sup>9</sup> is extremely important for the intranuclear chemodrug-sensitized radiation enhancement, which has not been reported yet.

Recent progress in nanotechnology has enabled successful syntheses of nuclear-targeting drug vehicles. For example, the small-sized (usually sub-50 nm) mesoporous nanoparticles (MSNs) conjugated with nuclear localization signal (NLS) ligands (such as TAT) may be efficiently transported into the cell nucleus.<sup>10</sup> However, the reported intranuclear drug delivery was

<sup>a</sup>State Key Laboratory of High Performance Ceramics and Superfine Microstructures, Shanghai Institute of Ceramics, Chinese Academy of Sciences, Shanghai, 200050, P. R. China. E-mail: wbbu@mail.sic.ac.cn; jlshi@mail.sic.ac.cn

<sup>b</sup>Institute of Radiation Medicine, Fudan University, Shanghai, 200032, P. R. China

<sup>c</sup>Department of Radiation Oncology, Shanghai Huadong Hospital, Fudan University, Shanghai, 200040, P. R. China

<sup>d</sup>Department of Radiology, Shanghai Cancer Hospital, Fudan University, Shanghai, 200032, P. R. China

† Electronic supplementary information (ESI) available: Experimental procedures, supplementary figures and preliminary evaluation of radiosensitization of MMC. See DOI: 10.1039/c4sc03080j



only achieved on the cellular level for the single mode of chemotherapy; it was not a theranostic that combined simultaneous bioimaging and multi-mode synergetic therapy. Recently, upconversion nanoparticles (UCNPs)<sup>11</sup> have been developed as magnetic/upconversion luminescent (MR/UCL) bimodal imaging probes due to their unique physical/chemical properties.<sup>12</sup> Therefore, the integration of UCNPs and nuclear-targeting MSNs may simultaneously achieve accurate imaging guidance and efficient intranuclear drug delivery for substantially enhanced chemo-/radiotherapy.<sup>13</sup>

In this study, a sub-50 nm nuclear-targeting rattle-structured upconversion core/mesoporous silica nanotheranostic system was firstly designed to directly deliver MMC into the nucleus for greatly enhanced damaging of the DNA with the assistance of X-ray irradiation. More importantly, we develop a new theranostic technique of “intranuclear radiosensitization”, which means that the MMC molecules released into the nucleoplasm may not only efficiently break down the intranuclear DNA, but also effectively enhance the radiotherapy efficacy due to the intranuclear chemodrug-sensitized radiation enhancement effects (Fig. 1). Therefore, our synthesized nuclear-targeting nanotheranostics are expected to achieve substantially enhanced intranuclear synergetic chemo-/radiotherapy under the monitoring of MR/UCL bimodal imaging, which may represent a significant step forward in the development of high-performance cancer theranostic upconversion nanoparticles.

## 2 Results and discussion

### 2.1 Synthesis and characterization of nuclear-targeting nanotheranostics

The sub-50 nm rattle-structured nanocomposites are usually not easy to synthesize because of the difficulties in controlling various

reaction parameters (*e.g.*, reaction time, TEOS addition amounts, *etc.*).<sup>14</sup> Herein, two chemical routes were used to fabricate the sub-50 nm nuclear-targeting nanotheranostics (Fig. 2a). In the first route, uniform hexagonal phase UCNPs (NaYF<sub>4</sub>:Yb/Er/Tm/Gd) were synthesized using the traditional thermal decomposition method (Fig. S1 and 2†). Then a thickness-controlled dense silica plus mesoporous silica shell was subsequently coated onto the UCNPs (denoted as UCNPs@SiO<sub>2</sub>@mSiO<sub>2</sub>).<sup>15</sup> In the second route, the UCNPs were transferred to a water phase by treatment in a pH = 4 aqueous solution of HCl,<sup>16</sup> followed by depositing a thickness-controlled mesoporous silica shell onto the ligand-free UCNPs (denoted as UCNPs@mSiO<sub>2</sub>).<sup>17</sup> Finally, by etching the intermediate dense silica or mesoporous silica with polyvinyl pyrrolidone (PVP) protecting the outer surface, the final sub-50 nm rattle-structured upconversion core/mesoporous silica nanotheranostics (RUMSNs) were successfully prepared. The transmission electron microscopy (TEM) characterizations (Fig. 2b–g) demonstrate the high dispersity of the products synthesized in each reaction, which meets the requirements of biomedical administrations.

It is worth mentioning that, different from the first chemical route reported in our previous study,<sup>8b</sup> the second chemical route has unique advantages in controlling the size of the sub-50 nm RUMSNs more easily and accurately in which only the thickness of the mesoporous silica shell is necessary to regulate, as compared to the need for tuning both the thickness of the dense silica and the mesoporous silica in the first route. Secondly, by the second route, a much shorter time period is needed for synthesizing the RUMSNs as compared to the time-

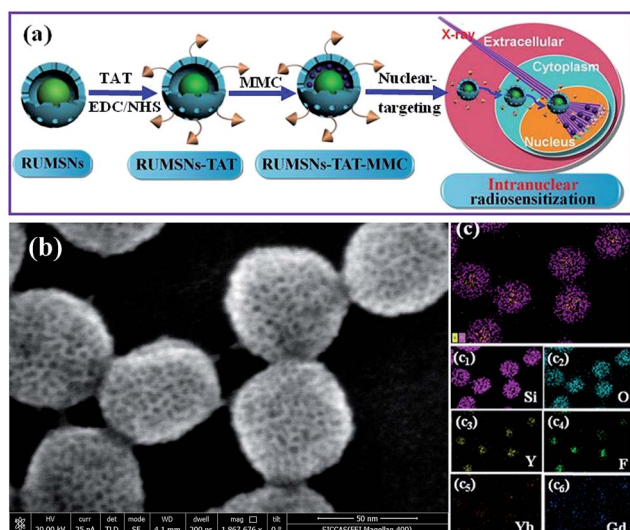


Fig. 1 (a) Schematic illustration of intranuclear radiosensitization. (b) Scanning electron microscopy (SEM) image of rattle-structured upconversion core/mesoporous silica nanotheranostics (RUMSNs). (c) Scanning transmission electron microscopy (STEM) image and the corresponding element mappings of the RUMSNs: (c<sub>1</sub>) Si; (c<sub>2</sub>) O; (c<sub>3</sub>) Y; (c<sub>4</sub>) F; (c<sub>5</sub>) Yb; (c<sub>6</sub>) Gd.

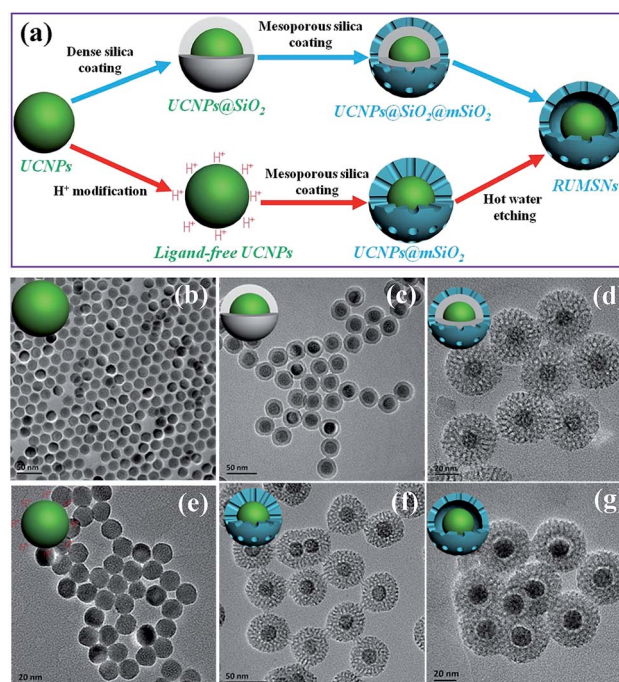


Fig. 2 (a) Schematic diagram of the two synthetic routes to RUMSNs. (b–g) TEM images of the products: (b) UCNPs; (c) UCNPs@SiO<sub>2</sub>; (d) UCNPs@SiO<sub>2</sub>@mSiO<sub>2</sub>; (e) ligand-free UCNPs; (f) UCNPs@mSiO<sub>2</sub>; (g) RUMSNs. The core, shell and overall sizes of RUMSNs are about 19, 10 and 47 nm, respectively.





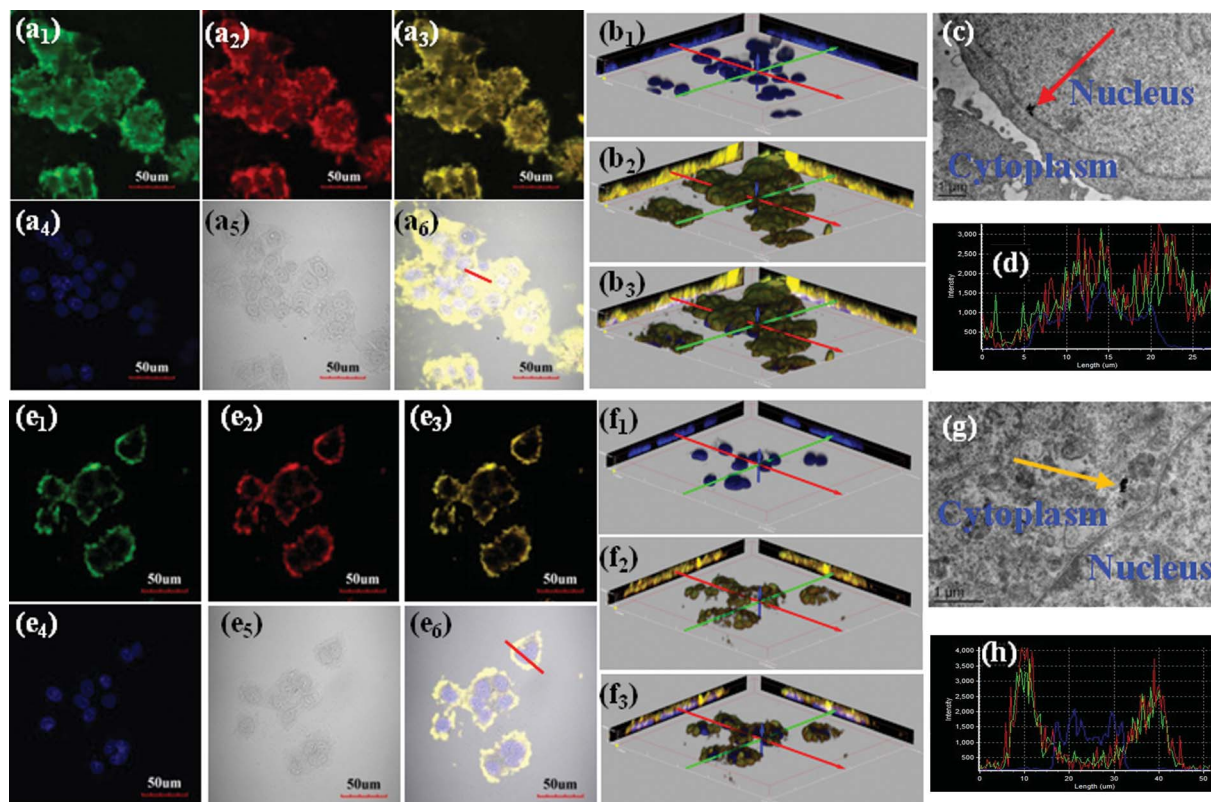


Fig. 3 (a<sub>1-6</sub> & e<sub>1-6</sub>) Confocal laser scanning microscopy (CLSM) imaging of MCF-7 cells incubated with (a<sub>1-6</sub>) the RUMSNs-TAT and (e<sub>1-6</sub>) the RUMSNs for 24 h. Blue luminescence is from the nucleus after being stained with DAPI. Upon NIR excitation, the RUMSNs emit yellow luminescence (merge of green/red luminescence). (b<sub>1-3</sub> & f<sub>1-3</sub>) The three-dimensional confocal luminescence reconstructions of MCF-7 cells incubated with (b<sub>1-3</sub>) the RUMSNs-TAT and (f<sub>1-3</sub>) the RUMSNs for 24 h. (c & g) Bio-TEM images of MCF-7 cells incubated with (c) the RUMSNs-TAT and (g) the RUMSNs for 24 h. Red arrow: the RUMSNs-TAT reside in the nucleus; yellow arrow: the RUMSNs reside in the cytoplasm. (d & h) Line-scanning profiles of luminescence intensity of the MCF-7 cells incubated with (d) the RUMSNs-TAT and (h) the RUMSNs for 24 h.

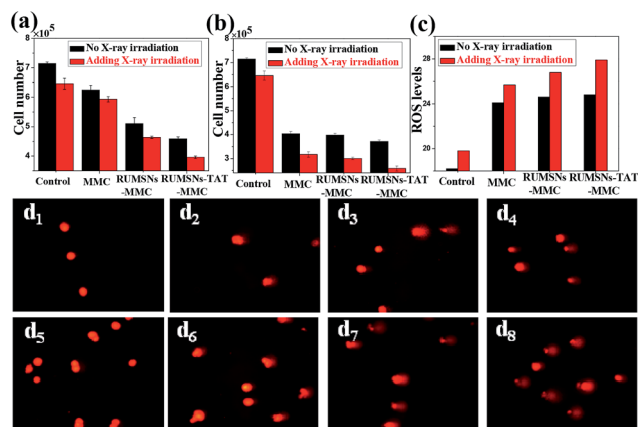


Fig. 4 (a & b) The viability of MCF-7 cells after different treatments for 24 h with an MMC concentration of (a)  $0.5 \mu\text{g mL}^{-1}$  and (b)  $10 \mu\text{g mL}^{-1}$ . (c) The ROS generation monitored by 2,7-dichlorofluorescein (DCF) luminescence for MCF-7 cells after different treatments. (d<sub>1-8</sub>) Direct observation of DNA breakdown using comet assays on MCF-7 cells after different treatments: (d<sub>1</sub>) control, (d<sub>2</sub>) MMC, (d<sub>3</sub>) RUMSNs-MMC, (d<sub>4</sub>) RUMSNs-TAT-MMC, (d<sub>5</sub>) RT, (d<sub>6</sub>) MMC + RT, (d<sub>7</sub>) RUMSNs-MMC + RT, and (d<sub>8</sub>) RUMSNs-TAT-MMC + RT. [MMC] =  $10 \mu\text{g mL}^{-1}$ .

further confirms that the highest cytotoxicity is achieved by the RUMSNs-TAT-MMC + RT due to the intranuclear chemodrug-sensitized radiation enhancement effects.

The substantially increased treatment efficiency and radiation enhancement effects are believed to be caused by the more severe DNA damage, as supported by the single-cell gel electrophoresis (comet assay) study (Fig. 4d & S11b<sup>†</sup>). The control group shows negligible DNA damage while long tails of stain can be observed in the nucleus after certain treatments, which indicates obvious DNA damage. As compared to the other treatments, the RUMSNs-TAT-MMC + RT has caused the most significant DNA damage (as evidenced by the longest tail), which further confirms the strongest radiation enhancement effects produced by the substantially enhanced synergistic chemo/radiotherapy in the nucleus as well as the much better therapeutic effects achieved by the intranuclear radiosensitization than the intracytoplasmic or extracellular radiosensitization.

The widespread multi-drug resistance (MDR) of malignant tumors is one of the major reasons for cancer treatment failure. With single-mode chemotherapy, satisfactory treatment is usually not achievable, which highlights the demand for the combination of chemotherapy with other therapeutic modes such as radiotherapy. We performed the same *in vitro*





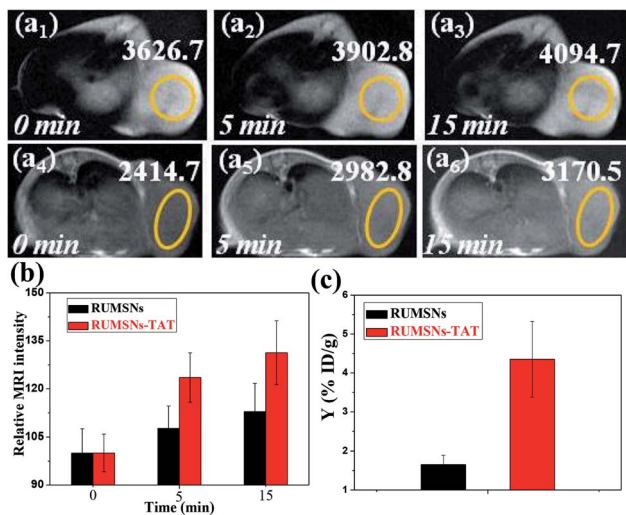


Fig. 7 (a) *In vivo* T<sub>1</sub>-MRI images of MCF-7 tumor-bearing mice after intravenous injection of (a<sub>1–3</sub>) the RUMSNs and (a<sub>4–6</sub>) the RUMSNs-TAT at designated time points. (b) Comparison of the MRI signal intensity of MCF-7 tumors after intravenous injection of the RUMSNs/RUMSNs-TAT at different time points. (c) Quantitative analysis of the Yttrium concentrations in tumors following the intravenous injection of the RUMSNs and RUMSNs-TAT.

also evidenced by the quantitative analysis in Fig. 7c. Therefore, the RUMSNs-TAT may be developed as magnetic imaging probes to localize to the tumor sites.

Thirdly, we carried out the *in vivo* therapy experiments on MCF-7 tumor-bearing nude mice. As seen from the bio-distribution study in Fig. 7c & S20,† much more RUMSNs-TAT (~4.35% ID Y g<sup>-1</sup>) can accumulate in tumors than RUMSNs (~1.65% ID Y g<sup>-1</sup>), which may be attributed to the unique function of TAT in penetrating blood vessels/cell membranes and achieving relatively higher retention within tumor cells.<sup>19</sup> In addition, the histological analysis of the tumors by low-resolution CLSM imaging (Fig. S21†) shows that much stronger green luminescence of RUMSNs-TAT (Fig. S21a<sub>2</sub>†) is observed in tumors, which further evidences the greater accumulation of the RUMSNs-TAT than the RUMSNs. More importantly, the green luminescence of the RUMSNs-TAT clearly localises at the nucleus of most tumor cells (Fig. S21a<sub>3</sub>†), which undoubtedly confirms that the RUMSNs-TAT can reach the nucleus of tumor cells with the assistance of TAT and achieve the intranuclear drug delivery *in vivo* following intravenous injection.

As compared to the control group, the tumors treated with the RUMSNs-TAT-MMC demonstrate more significant growth delay than those treated with the RUMSNs-MMC (Fig. 8a and b) due to the higher chemotherapeutic efficacy based on the intranuclear drug delivery rather than the intracytoplasmic delivery. With the assistance of X-ray irradiation, the synergetic chemo-/radiotherapy based on radiosensitization produces much better therapeutic effects than individual chemotherapy or radiotherapy. Similarly, the RUMSNs-TAT-MMC + RT can most effectively inhibit the tumor growth in half a month and produce much better therapeutic effects than the RUMSNs-MMC + RT, which may be attributed to the much more

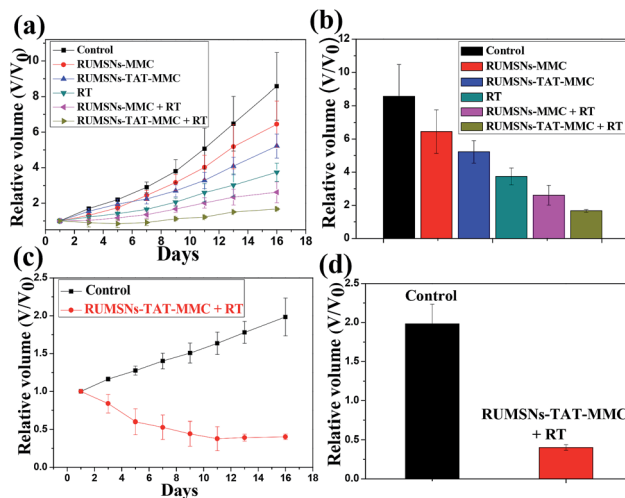


Fig. 8 (a) Tumor growth curves of MCF-7 tumor-bearing mice over a period of half a month after the corresponding treatments. (b) Relative MCF-7 tumor volumes of different groups after half a month of the corresponding treatments. (c) Tumor growth curves of MCF-7/ADR tumor-bearing mice over a period of half a month after treatment with the intranuclear radiosensitization. (d) Relative MCF-7/ADR tumor volumes after half a month of therapy with the intranuclear radiosensitization.

substantially enhanced chemo-/radiotherapy efficacy caused by the intranuclear radiosensitization than the intracytoplasmic radiosensitization, as can be clearly seen from the corresponding digital photos of tumors in Fig. S22.† Moreover, the tumors treated with the RUMSNs-TAT-MMC + RT demonstrate the most significant necrosis (as evidenced by images of hematoxylin-eosin (H & E) stained tumor sections in Fig. S23†), which further confirms the higher treatment efficiency and better radiation enhancement effects caused by the intranuclear radiosensitization in comparison to other kinds of therapies.

Finally, by implanting MCF-7/ADR cells into the right axilla of nude mice, we further estimated the therapeutic effects of the intranuclear radiosensitization on the MDR tumors. Surprisingly, the treatment with the RUMSNs-TAT-MMC + RT not only completely inhibits the growth of MCF-7/ADR tumors, but also leads to significant tumor regression by about 60% (Fig. 8c and d and as also clearly evidenced by the corresponding digital photos and H & E stained tumor sections in Fig. S24†), which marks one of the most significant instances in which the intranuclear radiosensitization provides a more advanced way for reversing MDR *in vivo*.

### 3 Conclusions

In summary, we have presented a new technique of “intranuclear radiosensitization” by designing a sub-50 nm multifunctional nuclear-targeting nanotheranostic system (RUMSNs-TAT) to directly deliver the radiosensitive chemotherapeutic drug MMC into the nucleus for the greatly elevated intranuclear chemodrug-sensitized radiation enhancement effects on damaging the DNA under high energy X-ray



irradiation. The *in vitro* and *in vivo* therapy experiments undoubtedly demonstrate the much more enhanced treatment efficiency by the intranuclear radiosensitization than the extracellular radiosensitization and intracytoplasmic radiosensitization in killing cancer cells and inhibiting tumor growth. Moreover, as the ATP level/P-gp expression can be significantly down-regulated by the nuclear-targeting nanotheranostics to bypass efflux action, the intranuclear radiosensitization also demonstrates remarkable advantages in efficiently reversing MDR and regressing the MDR tumor growth. Finally, based on the MR/UCL bimodal imaging performance, our synthesized nanotheranostics may be developed as the next generation of accurate imaging guided nuclear-targeting nanomedicine in the future.

## Acknowledgements

This work has been financially supported by the National Natural Science Foundation of China (Grant no. 51372260, 51132009, 21172043, 51102259) and the Shanghai Rising-Star Program (Grant no. 12QH1402500).

## Notes and references

- (a) J. Shen, Q. He, Y. Gao, J. Shi and Y. Li, *Nanoscale*, 2011, **3**, 4314; (b) Q. He, Y. Gao, L. Zhang, Z. Zhang, F. Gao, X. Ji, Y. Li and J. Shi, *Biomaterials*, 2011, **32**, 7711; (c) X. Duan, J. Xiao, Q. Yin, Z. Zhang, H. Yu, S. Mao and Y. Li, *ACS Nano*, 2013, **7**, 5858.
- (a) L. S. Jabr-Milane, L. E. van Vlerken, S. Yadav and M. M. Amiji, *Cancer Treat. Rev.*, 2008, **34**, 592; (b) H. Lage, *Cell. Mol. Life Sci.*, 2008, **65**, 3145; (c) M. F. Ullah, *Asian Pac. J. Cancer Prev.*, 2008, **9**, 1; (d) J. Gao, S.-S. Feng and Y. Guo, *Nanomedicine*, 2012, **7**, 465.
- (a) P. Juzenas, W. Chen, Y.-P. Sun, M. A. N. Coelho, R. Generalov, N. Generalova and I. L. Christensen, *Adv. Drug Delivery Rev.*, 2008, **60**, 1600; (b) W. P. Hogle, *Semin. Oncol. Nurs.*, 2006, **22**, 212.
- (a) J. F. Hainfeld, F. A. Dilmanian, D. N. Slatkin and H. M. Smilowitz, *J. Pharm. Pharmacol.*, 2008, **60**, 977; (b) P. Wardman, *Clin. Oncol.*, 2007, **19**, 397; (c) T. Nakae, Y. Uto, M. Tanaka, H. Shibata, E. Nakata, M. Tominaga, H. Maezawa, T. Hashimoto, K. L. Kirk, H. Nagasawa and H. Hori, *Bioorg. Med. Chem.*, 2008, **16**, 675.
- (a) K. A. Kennedy, S. Rockwell and A. C. Sartorelli, *Cancer Res.*, 1980, **40**, 2356; (b) M. Tomasz, *Chem. Biol.*, 1995, **2**, 575.
- C. Grau, J. P. Agarwal, K. Jabeen, A. R. Khan, S. Abeyakoon, T. Hadjieva, I. Wahid, S. Turkan, H. Tatsuzaki, K. A. Dinshaw and J. Overgaard, *Radiother. Oncol.*, 2003, **67**, 17.
- (a) U. Kulka, M. Schaffer, A. Siefert, P. M. Schaffer, A. Ölsner, K. Kasseb, A. Hofstetter, E. Dühmke and G. Jori, *Biochem. Biophys. Res. Commun.*, 2003, **311**, 98; (b) B. T. Hill, R. D. H. Whelan, S. A. Shellard, S. McClean and L. K. Hosking, *Invest. New Drugs*, 1994, **12**, 169; (c) P. G. Rose, B. N. Bundy, E. B. Watkins, J. T. Thigpen, G. Deppe, M. A. Maiman, D. L. Clarke-Pearson and S. Insalaco, *N. Engl. J. Med.*, 1999, **340**, 1144.
- (a) M. E. Werner, J. A. Copp, S. Karve, N. D. Cummings, R. Sukumar, C. Li, M. E. Napier, R. C. Chen, A. D. Cox and A. Z. Wang, *ACS Nano*, 2011, **5**, 8990; (b) W. Fan, B. Shen, W. Bu, F. Chen, K. Zhao, S. Zhang, L. Zhou, W. Peng, Q. Xiao, H. Xing, J. Liu, D. Ni, Q. He and J. Shi, *J. Am. Chem. Soc.*, 2013, **135**, 6494.
- J.-n. Liu, W. Bu, L.-m. Pan, S. Zhang, F. Chen, L. Zhou, K.-l. Zhao, W. Peng and J. Shi, *Biomaterials*, 2012, **33**, 7282.
- L. Pan, Q. He, J. Liu, Y. Chen, M. Ma, L. Zhang and J. Shi, *J. Am. Chem. Soc.*, 2012, **134**, 5722.
- (a) J. Zhou, Z. Liu and F. Li, *Chem. Soc. Rev.*, 2012, **41**, 1323; (b) Z. Gu, L. Yan, G. Tian, S. Li, Z. Chai and Y. Zhao, *Adv. Mater.*, 2013, **25**, 3758; (c) T. Cao, Y. Yang, Y. Gao, J. Zhou, Z. Li and F. Li, *Biomaterials*, 2011, **32**, 2959; (d) T. Cao, T. Yang, Y. Gao, Y. Yang, H. Hu and F. Li, *Inorg. Chem. Commun.*, 2010, **13**, 392; (e) G. Chen, J. Shen, T. Y. Ohulchanskyy, N. J. Patel, A. Kutikov, Z. Li, J. Song, R. K. Pandey, H. Agren, P. N. Prasad and G. Han, *ACS Nano*, 2013, **6**, 8280; (f) J. Shen, G. Chen, A.-M. Vu, W. Fan, O. S. Bilsel, C.-C. Chang and G. Han, *Adv. Opt. Mater.*, 2013, **1**, 644; (g) J. Shen, G. Chen, T. Y. Ohulchanskyy, S. J. Kesseli, S. Buchholz, Z. Li, P. N. Prasad and G. Han, *Small*, 2013, **9**, 3213; (h) A. Punjabi, X. Wu, A. Tokatli-Apollon, M. El-Rifai, H. Lee, Y. Zhang, C. Wang, Z. Liu, E. M. Chan, C. Duan and G. Han, *ACS Nano*, 2014, **8**, 10621.
- (a) F. Chen, W. Bu, S. Zhang, X. Liu, J. Liu, H. Xing, Q. Xiao, L. Zhou, W. Peng, L. Wang and J. Shi, *Adv. Funct. Mater.*, 2011, **21**, 4285; (b) F. Chen, W. Bu, S. Zhang, J. Liu, W. Fan, L. Zhou, W. Peng and J. Shi, *Adv. Funct. Mater.*, 2013, **23**, 298; (c) Y. I. Park, H. M. Kim, J. H. Kim, K. C. Moon, B. Yoo, K. T. Lee, N. Lee, Y. Choi, W. Park, D. Ling, K. Na, W. K. Moon, S. H. Choi, H. S. Park, S.-Y. Yoon, Y. D. Suh, S. H. Lee and T. Hyeon, *Adv. Mater.*, 2012, **24**, 5755; (d) J. Zhou, Y. Sun, X. Du, L. Xiong, H. Hu and F. Li, *Biomaterials*, 2010, **31**, 3287.
- (a) C. Li, Z. Hou, Y. Dai, D. Yang, Z. Cheng, P. a. Ma and J. Lin, *Biomater. Sci.*, 2013, **1**, 213; (b) J. Liu, W. Bu, S. Zhang, F. Chen, H. Xing, L. Pan, L. Zhou, W. Peng and J. Shi, *Chem.-Eur. J.*, 2012, **18**, 2335.
- Y. Hu, Q. Zhang, J. Goebel, T. Zhang and Y. Yin, *Phys. Chem. Chem. Phys.*, 2010, **12**, 11836.
- N. M. Idris, M. K. Gnanasammandhan, J. Zhang, P. C. Ho, R. Mahendran and Y. Zhang, *Nat. Med.*, 2012, **18**, 1580.
- N. Bogdan, F. Vetrone, G. A. Ozin and J. A. Capobianco, *Nano Lett.*, 2011, **11**, 835.
- J. Liu, W. Bu, L. Pan and J. Shi, *Angew. Chem., Int. Ed.*, 2013, **52**, 4375.
- Y. Gao, Y. Chen, X. Ji, X. He, Q. Yin, Z. Zhang, J. Shi and Y. Li, *ACS Nano*, 2011, **5**, 9788.
- (a) H. Yuan, A. M. Fales and T. Vo-Dinh, *J. Am. Chem. Soc.*, 2012, **134**, 11358; (b) P. Wunderbaldinger, L. Josephson and R. Weissleder, *Bioconjugate Chem.*, 2002, **13**, 264; (c) V. P. Torchilin, *Adv. Drug Delivery Rev.*, 2008, **60**, 548.

